Scientific Research and Essays Vol. 7(30), pp. 2718-2730, 2 August, 2012
Available online at http://www.academicjournals.org/SRE
DOI: 10.5897/SRE11.2196
ISSN 1992-2248 ©2012 Academic Journals

Full Length Research Paper

A novel adaptive color to grayscale conversion algorithm for digital images

Wei Hong Lim and Nor Ashidi Mat Isa*

School of Electrical and Electronic Engineering, Engineering Campus, Universiti Sains Malaysia, 14300 Nibong Tebal, Penang, Malaysia.

Accepted 6 July, 2012

A color image sent to the monochrome device must undergo the color-to-grayscale conversion process. Although the conventional color-to-grayscale conversion algorithms are widely used, their performance is questionable in certain circumstances and poor quality resultant grayscale images will be produced. This paper tackled some drawbacks of the conventional methods by introducing a novel approach namely the Adaptive Color to Grayscale (ACGS) conversion algorithm. In the proposed ACGS method, the pixels distribution analysis of input color images was performed to calculate the weight contribution of red, green, and blue components during the conversion process. The extensive experimental results demonstrated the superior qualitative and quantitative performance of the proposed ACGS method over the conventional algorithms and its feasibility in real-time video processing applications. These promising results suggest that the proposed ACGS method is suitable to be employed in the monochrome devices for pre- and post- processing of digital images.

Key words: Color-to-grayscale conversion, adaptive, color image, grayscale image, image pre-processing.

INTRODUCTION

Color-to-grayscale conversion process is one of the most important functions for monochrome devices to produce grayscale output images. This is known as a dimensional reduction process as the color image with three dimensional color information (24-bit) is reduced into one dimension of the grayscale representation (8-bit) (Bala and Eschbach, 2004; Cadik, 2008).

Despite the advancement and the ever increasing popularity of the low-cost polychrome devices (e.g. color printer), the use of monochrome devices such as the grayscale printer and grayscale scanner still remains to be widespread (Bala and Eschbach, 2004; Rasche et al., 2005). This is because the 24-bit color images take more storage space and slower data transmission rate, which leads to the higher cost of color photocopies or printouts as compared to the grayscale counterpart (Kekre and Thepade, 2009). For practical consideration, it is more cost-effective to minimize the information into 8-bit grayscale images as they take less memory space for storage and shorter time for data transmission. Figure 1 illustrates the high level block diagram of a computer system that is adopted to carry out the conversion process. As shown in Figure 1, the monitor of red, green, and blue (RGB) values are converted into the printer's grayscale using the appropriate conversion procedure. The resultant grayscale images produced can be used for many purposes, such as printed textbooks and catalogues, legacy recognition systems, the stylization of video, medical display, etc. (Smith et al., 2008; Gooch et

*Corresponding author. E-mail: ashidi@eng.usm.my. Tel: +604 5996051.

Abbreviations: 2-D, Two-dimensional; **3-D,** three dimensional; **ACGS,** adaptive color to grayscale; **AE,** average entropy; **AMI,** average mean intensity; **ASD,** average standard deviation; **E,** entropy; **HSV,** human visual system; **MI,** mean intensity; **NTSC,** national television system committee; **PDF,** probability density function; **RGB,** red, green, and blue; **SD,** standard deviation.

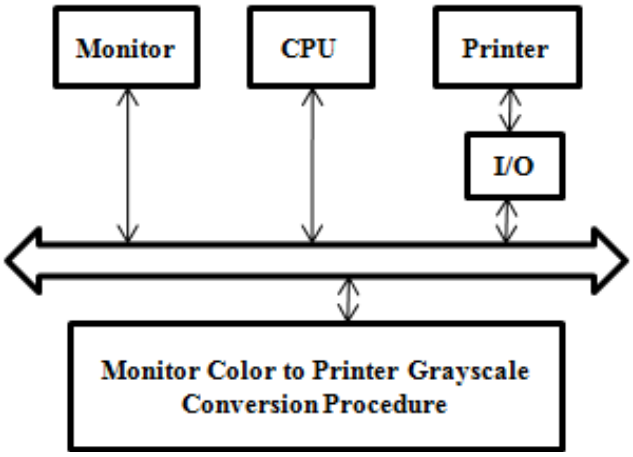

Figure 1. High level block diagram of the computer system adopted to carry out the color-to-grayscale conversion process.

al., 2008; Grundland and Dodgson, 2007).

In addition, the color-to-grayscale conversion process is also widely used in the machine vision systems such as, the face recognition system. The resultant grayscale images produced are subjected to the subsequent higher levels of processing steps such as edge detection, segmentation, feature extraction, etc. (Gonzalez and Woods, 2002) as most of the current available image processing techniques are developed based on the grayscale images (Gooch et al., 2005; Cadik, 2008). The generalization of these grayscale image processing techniques into their counterpart of color images processing techniques is not trivial as there are more attributes required to represent a color image (that is, hue, saturation, and intensity) than the grayscale image (that is, intensity). In order to enable the subsequent step of processing, the resultant grayscale images produced must possess the high quality characteristic in terms of the brightness, contrast, and amount of details revealed.

In this paper, the color-to-grayscale conversion algorithm based on the RGB color model will be developed as most of the displays and printing systems store the color images in the RGB format. Conventionally, the Averaging and National Television System Committee (NTSC) methods are two widely used conversion techniques in the RGB space (Rashe et al., 2005; Gooch et al., 2005; Dikbas et al., 2007). Both of these conventional methods employ the linearly weighed transformation approach, where the constant weight contribution values will be assigned to red (R), green (G), and blue (B) components of input color images respectively, during the conversion process.

Consider an input color image, *I* and let the *R*(*x, y*), *G*(*x, y*), and *B*(*x, y*) represent the red, green, and blue color channels' intensity at the coordinate (*x*, *y*) respectively. The resultant grayscale image *J* can be determined by the linearly weighted transformation as follow:

$$J(x,y) = [a \times R(x,y)] + [b \times G(x,y)] + [c \times B(x,y)] \quad (1)$$

connotating that the values of *a*, *b*, and *c* represent the weight contribution values assigned to the R, G, and B channels respectively, during the conversion process.

For the NTSC method, it assigns different weights for different color components as this method takes into account the factors such as the relative spectral distribution of the color channels and human perception during the conversion process (Dikbas et al., 2007). The values of *a*, *b*, and *c* assigned to the R, G, and B components of a color image are 0.299, 0.587, and 0.144 respectively. These weights correspond to the sensitivity of the human visual system (HSV) for each of the RGB primaries (Gonzalez and Woods, 2002).

Unlike the NTSC method, the Averaging method does not consider the relative spectral power distribution of the RGB channels during the conversion process. The resultant grayscale intensity level produced by this method is the mean of the RGB channels, where the weight contribution assigned to R, G, and B components are the same and constant, that is, $a = b = c = \frac{1}{3}$.

In general, both of the above mentioned conventional methods perform well in non-specialized uses. However, their performances become questionable when certain circumstances, that is the single dominant color and low illumination color images are met. Single dominant color and low illumination color images referring to color images with the pixel distribution are strongly biased to certain color components and low intensity levels respectively. The failure of these conventional methods is due to the constant weight contribution that is assigned to the R, G, and B components during the conversion process. For example, the NTSC method has failed in the

single-view face recognition system as the human skin color pixels' distributions are strongly biased to red (Lu and Plataniotis, 2009). As the NTSC method assigns low weight contribution to the red component, the dominant component of human skin (that is, red) is suppressed, and many important features of an input image might be hidden. This results in the condition that a weakened grayscale face signal is produced, which usually has low level of brightness and interpretability. These drawbacks might lead to the risk of reduced recognition rates of the face recognition system. For the Averaging method, the loss of important visual cues of an original image is imminent (Bala and Eschbach, 2004; Gooch et al., 2005; Bala and Braun, 2004). A color document may look well distinguishable in color, however when printed in the grayscale format, the color with different hues but with the same luminance level will become undistinguishable in the grayscale.

Besides the above mentioned conventional methods, there are many state-of-art color-to-grayscale conversion algorithms that have been proposed recently (Bala and Eschbach, 2004; Rashe et al., 2005; Kekre and Thepade, 2009; Smith et al., 2008; Gooch et al., 2008; Grundland and Dodgson, 2007; Cadik, 2008; Dikbas et al., 2007; Lu and Plataniotis, 2009; Bala and Braun, 2004). These recently proposed algorithms employ various techniques such as providing the feedback of high frequency errors in the chromaticity component (Bala and Eschbach, 2004), solving optimization problem (Rashe et al., 2005; Gooch et al., 2008), etc. Such recently proposed algorithms, however, will not be used in comparison with our proposed algorithm in the following section. This is because the implementation of these state-of-the-art techniques are relatively complex, as they are not derived based on the linearly weighted transformation approach and the conversion process is not performed in the RGB color space.

In this paper, we propose a new Adaptive Color to Grayscale (ACGS) conversion algorithm to overcome the drawbacks of the conventional algorithms. Similar to the conventional methods, the proposed ACGS method employs the linearly weighted transformation approach and is developed in the RGB color space in order to preserve its nature of simple implementation. Unlike the conventional methods, the proposed ACGS method determines the weight contribution of R, G, and B components for a given color image adaptively. In this proposed ACGS method, an extensive pixels' distribution analysis of the input color image will be performed to calculate the weight contribution of R, G and B components during the conversion process.

MATERIALS AND METHODS

This section covers the details of the proposed ACGS method. In the proposed method, the effect of the scene illuminant on the input images will be taken into account before the weight contribution of R, G, and B components are determined. This is due to the fact that most of the digital imaging devices do not have the excellent color constancy ability as compared with the HVS. When the non-white illumination is present during the image capturing process, the image will be illuminated by the corresponding non-white illumination and will be prone to have higher intensity of the particular illuminant. For example, the object will appear reddish when illuminated by red illuminant. By converting the image using the constant weight contribution of R, G, and B components (that is, as in the NTSC and Averaging methods), an insignificant resultant grayscale image could be obtained especially if the dominant illumination color in the image is suppressed (that is, red color in the NTSC method). Thus, this study proposes to determine the degree of the illumination color percentage of a color image by analyzing the color pixel distribution of the input image. Based on the analysis result, the weight contribution of R, G, and B components will then be calculated adaptively.

In general, a color image can be represented by a three dimensional (3-D) RGB color space. In the proposed ACGS method, this 3-D RGB color space will be decomposed into three two-dimensional (2-D) color channel planes, namely the H_{RG} (r, g), H_{GB} (g, b), and H_{RB} (r, b) planes as illustrated in Figure 2. Each of them represents the pixels' distribution of red-green components, green-blue components, and red-blue components respectively, in terms of intensity levels. The values of r, g, and b represent the intensity level of the R, G, and B components respectively, ranging from 0 to 255. The centroid of the pixels' distribution in these three 2-D color channel planes are used as basic information for the weight contribution calculation for each color component.

As different color images have different distributions of R, G, and B components in terms of intensity level, the 2-D color channel planes produced are also different. For example, if the dominant component of a given color image is red, then the pixels' distribution in 2-D color channel planes of H_{RG} (r, g) and H_{RB} (r, b) will concentrate towards the r-axis. This is proven in the "Red Lanterns" as illustrated in Figure 3. Based on the visual inspection and the 3-D RGB color model as shown in Figure 3(b), it is observed that the dominant color of "Red Lanterns" is red and most of the color pixels are concentrated at the r-axis. This observation is supported by the three 2-D color channel planes as shown in Figures 3(c)-(e) where the pixel distributions in H_{RG} (r, g) and H_{RB} (r, b) planes are inclined towards the r-axis.

In the first step of the proposed ACGS method, the pixels distributions of the color image in terms of intensity levels for red-green, green-blue, and red-blue components are constructed in order to obtain the 2-D color channel planes of $H_{RG}(r, g)$, $H_{GB}(g, b)$, and $H_{RB}(r, b)$ for red-green, green-blue, and red-blue components, respectively.

Next, the centroid values of the pixels' distribution for each 2-D color channel plane are determined. The centroid values obtained for $H_{RG}(r, g)$, $H_{GB}(g, b)$, and $H_{RB}(r, b)$ planes are assigned as (r_{RG}, g_{RG}), (g_{GB}, b_{GB}), and (r_{RB}, b_{RB}) respectively, and can be determined based on:

For the H_{RG} (r, g) Plane:

$$r_{RG} = \frac{1}{A_{RG}} \sum_{r=0}^{255} rA_{(RG,\,r)} \tag{2}$$

$$g_{RG} = \frac{1}{A_{RG}} \sum_{g=0}^{255} gA_{(RG,\,g)} \tag{3}$$

For the H_{GB} (g, b) Plane:

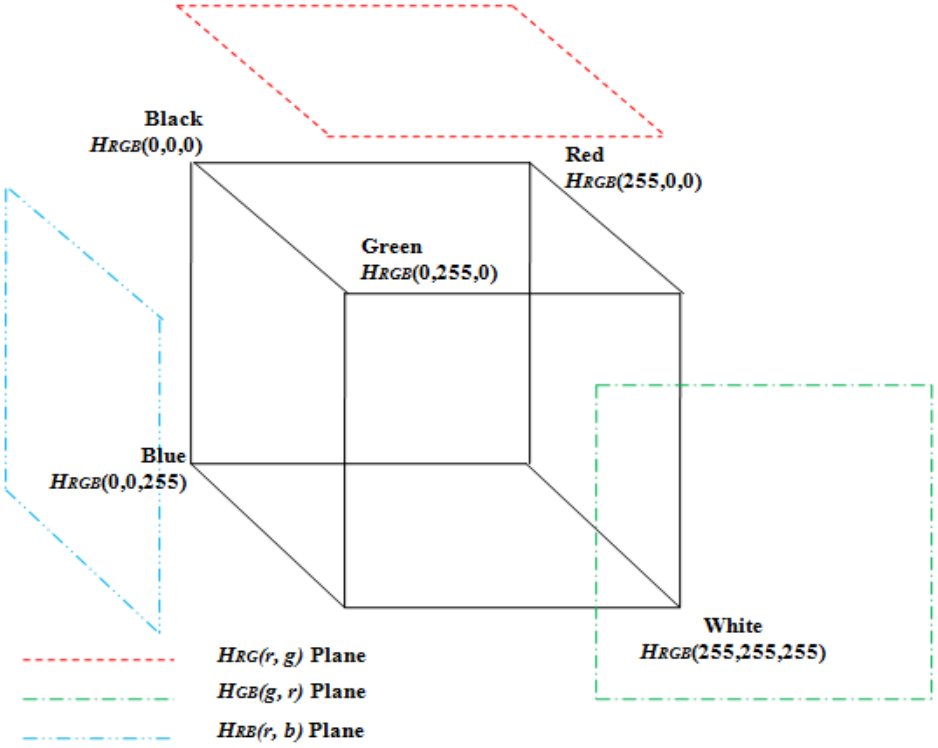

Figure 2. Decomposition of 3-D RGB color model, H_{RGB} (r, g, b) into three 2-D color channel planes of H_{RG} (r, g), H_{GB} (g, b), and H_{RB} (r, b).

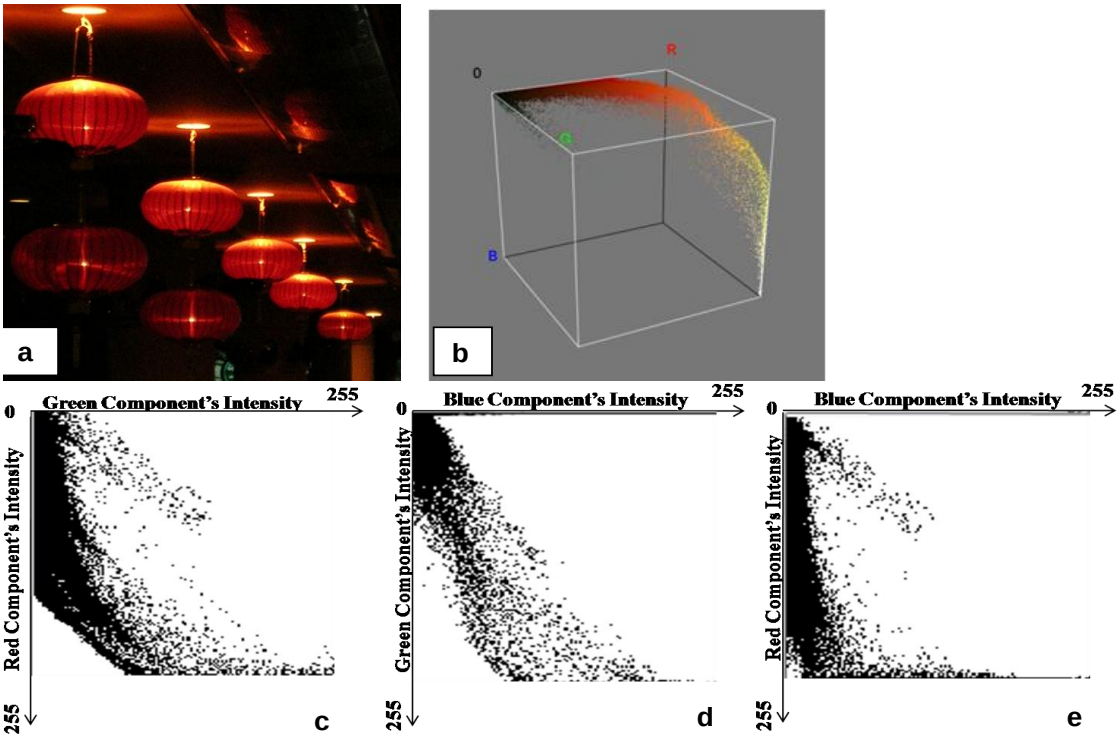

Figure 3. (a) "Red Lanterns" image. (b) 3-D RGB color model that represents the "Red Lanterns" image. (c) 2-D color channel plane of H_{RG}(r, g), (d) 2-D color channel plane of H_{GB}(g, b), and (e) 2-D color channel plane of H_{RB}(r, b).

$$g_{GB} = \frac{1}{A_{GB}} \sum_{g=0}^{255} gA_{(GB,\,g)} \quad (4)$$

$$b_{GB} = \frac{1}{A_{GB}} \sum_{b=0}^{255} bA_{(GB,\,b)} \quad (5)$$

For the H_{RB} (r, b) Plane:

$$r_{RB} = \frac{1}{A_{RB}} \sum_{r=0}^{255} rA_{(RB,\,r)} \quad (6)$$

$$b_{RB} = \frac{1}{A_{RB}} \sum_{b=0}^{255} bA_{(RB,\,b)} \quad (7)$$

where, $\sum_{r=0}^{255} rA_{(RG,\,r)}$ and $\sum_{g=0}^{255} gA_{(RG,\,g)}$ are the first moments of area of the r-axis and g-axis in the $H_{RG}(r,g)$ plane. $\sum_{g=0}^{255} gA_{(GB,\,g)}$ and $\sum_{b=0}^{255} bA_{(GB,\,b)}$ are the first moments of area in the g-axis and b-axis for the $H_{GB}(g,b)$ plane, while $\sum_{r=0}^{255} rA_{(RB,\,r)}$ and $\sum_{b=0}^{255} bA_{(RB,\,b)}$ are the first moments of area in the r-axis and b-axis for the $H_{RB}(r,b)$ plane. The values of $A_{(RG,\,r)}$, $A_{(RG,\,g)}$, $A_{(GB,\,g)}$, $A_{(GB,\,b)}$, $A_{(RB,\,r)}$ and $A_{(RB,\,b)}$ represent the elemental area measured from a given r-, g-, and b-axes of the $H_{RG}(r, g)$, $H_{GB}(g, b)$, and $H_{RB}(r, b)$ planes respectively. On the other hand, the values of A_{RG}, A_{GB}, and A_{RB} represent the total areas of the pixels' distribution in the $H_{RG}(r, g)$, $H_{GB}(g, b)$, and $H_{RB}(r, b)$ planes respectively.

Based on the centroid values obtained from Equation (2) to (7), the mean intensity level for each R, G, and B component (assigned as R_{mean}, G_{mean}, and B_{mean} respectively) is then calculated using:

$$R_{mean} = \frac{1}{2}\left(r_{RG} + r_{RB}\right) \quad (8)$$

$$G_{mean} = \frac{1}{2}\left(g_{RG} + g_{GB}\right) \quad (9)$$

$$B_{mean} = \frac{1}{2}\left(b_{GR} + b_{RB}\right) \quad (10)$$

Next, the proposed ACGS method will determine the weight contributions of R, G, and B components (designated as a, b and c respectively as shown in (1)) based on the values of R_{mean}, G_{mean}, and B_{mean}, as follow:

$$a = \frac{R_{mean}}{R_{mean} + G_{mean} + B_{mean}} \quad (11)$$

$$b = \frac{G_{mean}}{R_{mean} + G_{mean} + B_{mean}} \quad (12)$$

$$c = \frac{B_{mean}}{R_{mean} + G_{mean} + B_{mean}} \quad (13)$$

Finally, these a, b, and c values are substituted into (1) to convert each color pixel into its respective grayscale pixel. As shown in Equations (11) to (13), the color components with a higher mean intensity value will give a higher contribution during the conversion process. This explains the adaptive capability of the proposed ACGS method.

RESULTS AND DISCUSSION

In this paper, the capabilities of the proposed ACGS method are tested on two categories of color images, namely the single dominant color and low illumination color images. These two types of images are commonly produced during the image capturing process using the consumer digital still camera especially among amateur photographers. Two single dominant color images, namely "Red Lanterns" and "Fishes", and two low illumination color images, namely "Weave" and "Fruits" are selected to demonstrate the performance of the proposed algorithms. The performance of the proposed algorithms will be compared with the conventional methods, that is, the Averaging and NTSC methods. In addition, the video processing analysis is performed as well, to investigate the feasibility of the proposed ACGS method in the real-time video processing applications.

Qualitative analysis

The resultant images of "Red Lanterns", "Fishes", "Weave", and "Fruits" are illustrated in Figures 4 to 7 respectively. In each figure, the important visual findings that highlight the capabilities of the proposed ACGS method are highlighted by arrows.

Based on the visual inspections of "Red Lanterns", "Fishes", "Weave", and "Fruits" images as illustrated in Figures 4 to 7 respectively, the conventional methods do not perform well in the single dominant color and low illumination color images. All the resultant grayscale images produced have low brightness, as illustrated in images (b) and (c) of Figures 4 to 7. This is due to the constant weight contribution that is assigned to the R, G, and B components during the conversion process. The assignment of constant weight contribution may lead to the suppression of the dominant color component and enhancement of the non-dominant color component.

In addition, the resultant grayscale images produced by the Averaging and NTSC methods have low contrast and little amount of details revealed. This can be shown in "Red Lanterns", "Fishes", "Weave", and "Fruits" (represented by Figures 4 to 7 respectively). For "Red Lantern" as illustrated in Figure 4, it can be observed that the intensity levels of the bottom part of the lanterns and the background do not differ significantly. The edges of the bottom part of the lanterns are not properly preserved, leading to the bottom lanterns looking undistinguishable from the background. For the resultant

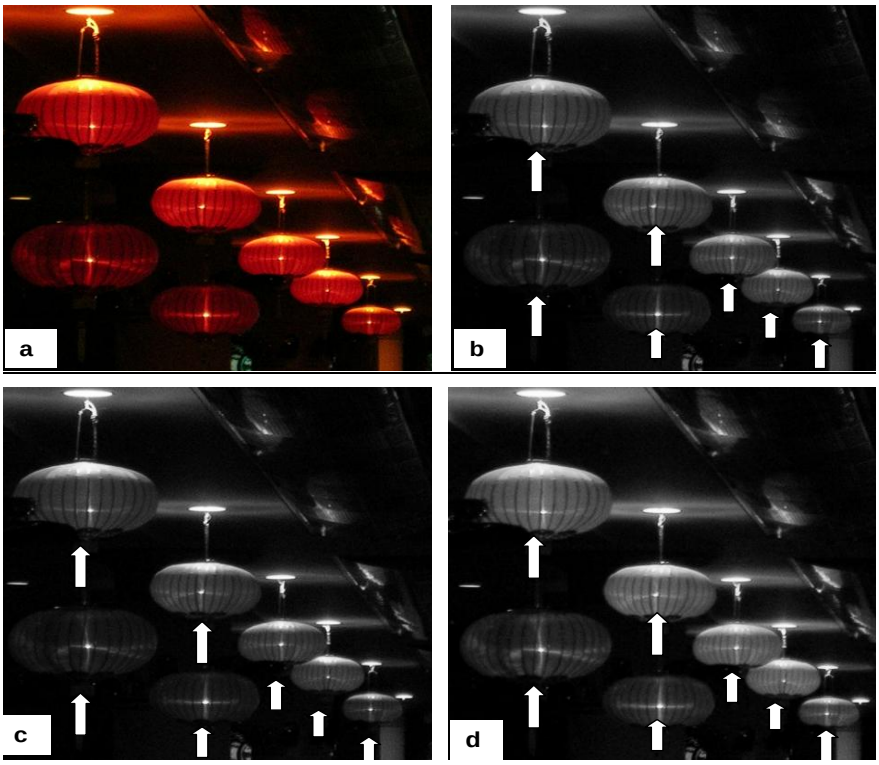

Figure 4. (a) Original "Red Lantern" image. The resultant grayscale images produced by (b) Averaging, (c) NTSC, and (d) ACGS methods.

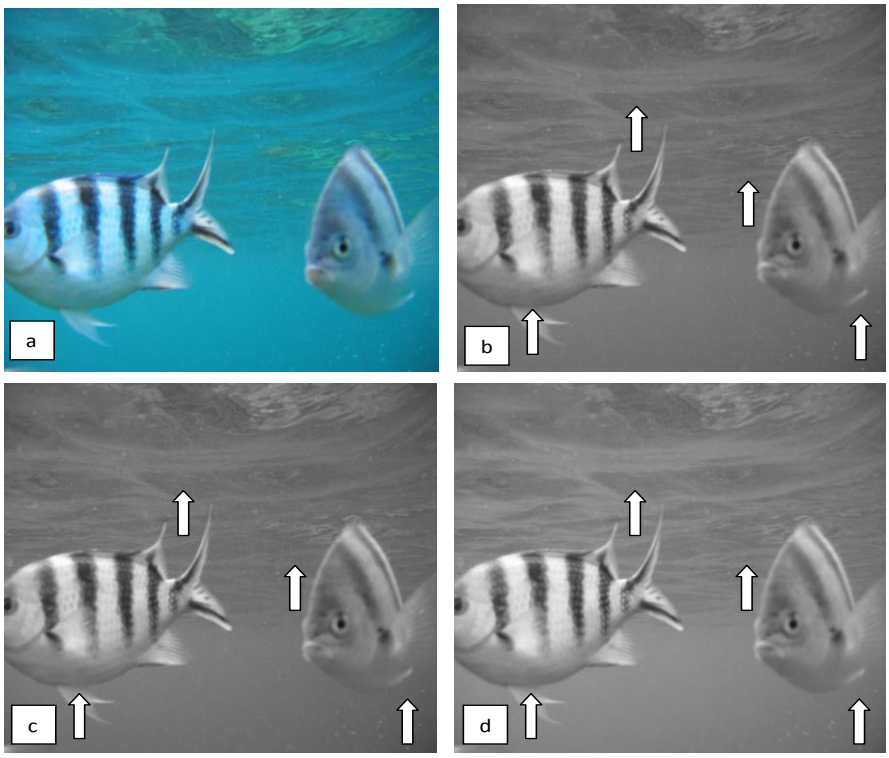

Figure 5. (a) Original "Fishes" image. The resultant grayscale images produced by (b) Averaging, (c) NTSC, and (d) ACGS methods.

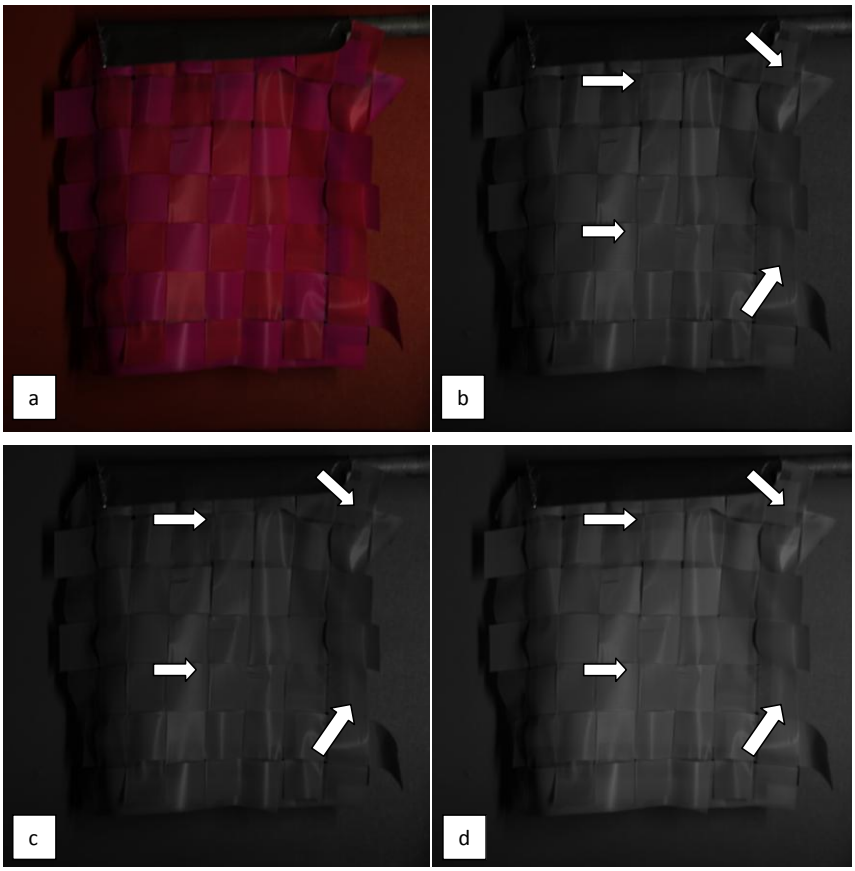

Figure 6. (a) Original "Weave" image. The resultant grayscale images produced by (b) Averaging, (c) NTSC, and (d) ACGS methods.

grayscale images of "Fishes" as illustrated in Figure 5, it can be observed that the difference in intensity levels between the bright part and the dark part at the background (that is, sea) is not significant. Thus, the patterns of wave are not clearly displayed. In addition, the body of fish at the right hand side is hardly distinguishable from the background as the edge of the fish is not sufficiently sharp. For the resultant grayscale images of "Weave" as illustrated in Figure 6, the contrast levels between the weave and the background of images are quite similar, which leads to the weave, the weave handle and the background being hardly distinguished from each other.

Finally, for the resultant grayscale images of "Fruits" as shown in Figure 7, the fruits at the left side of the image are hardly distinguished from each other as the fruits' edges are blurry. In addition, the shadows of the fruits are hardly separated from the background (that is, wall) due to the similarity of their intensity levels. As a conclusion, both the Averaging and NTSC methods perform poorly in the single dominant color and low illumination color images.

Meanwhile, the resultant grayscale images produced by the proposed ACGS method have shown improvement as compared to the conventional methods. Visually, the resultant grayscale images produced by the ACGS method have higher mean intensity than those produced by the Averaging and NTSC methods. This can be observed in all images (that is, "Red Lanterns", "Fishes", "Weave", and "Fruits" images) as illustrated in Figures 4 to 7. This is because the weight contribution of R, G, and B components in the ACGS method are determined in an adaptive procedure as compared to the conventional methods, where different weight contributions of R, G, and B components are assigned to different input color images. By employing this adaptive approach, the dominant component will always be assigned to the highest weight contribution and will never be suppressed.

In addition, the resultant grayscale images produced by the ACGS method have higher contrast and details contained than those produced by the conventional methods. In all the resultant grayscale images produced by the proposed ACGS method, the bright region becomes brighter and dark region becomes darker, indicating that the contrast of the grayscale images is significantly increased. In addition, the edges of the objects are successfully sharpened, thus, the objects are more distinguishable from the background. For "Red

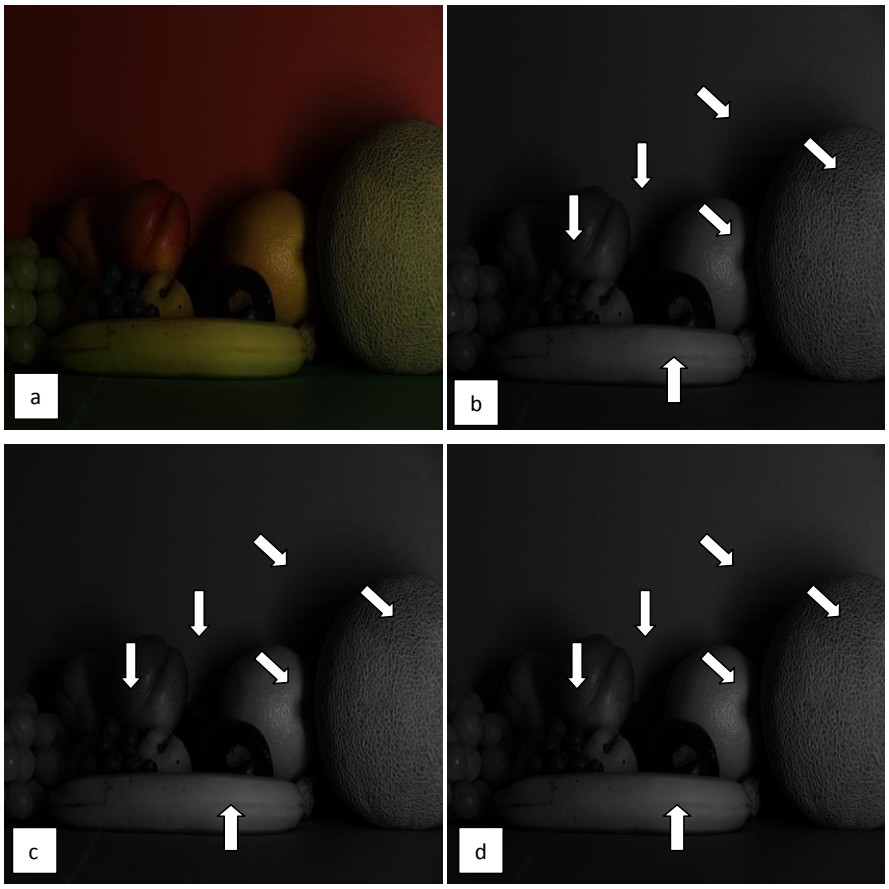

Figure 7. (a) Original “Fruits” image. The resultant grayscale images produced by (b) Averaging, (c) NTSC, and (d) ACGS methods.

Lanterns” as illustrated in Figure 4, two lanterns at the bottom part have higher contrast than those produced by the conventional methods as the difference in the intensity level between the red lanterns and the background are greater as compared to the conventional methods. This leads to the condition whereby the two lanterns at the bottom part are easier to be distinguished from the dark background. The proposed ACGS method is also capable in improving the contrast of “Fishes” as shown in Figure 5. The resultant grayscale images produced have improved contrast, especially at the background of the image (that is, sea) where the patterns of waves are clearly presented. Compared to the resultant grayscale images produced by the conventional methods as displayed in Figures 5 (b) and (c), the wave patterns details in Figure 5(d) produced by the ACGS method is highlighted substantially as the bright regions of the wave appear brighter, whilst the dark regions of the wave appear darker. In addition, for the fish at the right hand side, its body has intensity levels that are distinctive from the sea water, which outlines the fish from the background rather clearly. For “Weave” in Figure 6, the weave, the weave handler and the background can be easily distinguished due to the increase of contrast of images. In addition, the line patterns in the weave are clearly presented and this highlights the superior detail-preserving capability of the proposed ACGS method. Finally, for “Fruits” as illustrated in Figure 7, it can be observed that both the peaches at the left hand side can be distinguished from one another. In addition, all the fruits in the resultant grayscale image are more distinguishable from their shadows and background as the edges of all fruits are successfully sharpened. Furthermore, it can be observed that the background of the grayscale image produced by the proposed ACGS method (Figure 5(d)) provides a more pleasant visual experience to observer as it is brighter and has better contrast as compared to Figures 5(b) and (c) produced by the conventional methods. These observations further verify the capability of the proposed ACGS method in producing the grayscale images with better brightness and contrast.

Based on the results of the qualitative analysis, the resultant grayscale images produced by the proposed ACGS method have higher mean intensity, contrast, and amount of details revealed as compared to the

Table 1. Quantitative measurement for “Red Lanterns”, “Fishes”, “Weave”, and “Fruits” Images.

Algorithms	Red Lanterns			Fishes			Weave			Fruits		
	MI	SD	E(bits)	MI	SD	E(bits)	MI	SD	E(bits)	MI	SD	E(bits)
Averaging	22	33.8897	5.73998	117	**24.4955**	6.13986	28	14.3621	5.72865	21	14.6011	5.70009
NTSC	22	35.7416	5.76007	116	23.7504	6.12199	25	12.2581	5.53546	23	16.4037	5.78467
ACGS	**31**	**43.6460**	**6.13089**	**131**	24.0628	**6.23286**	**38**	**18.8905**	**6.09749**	**25**	**16.4092**	**5.90912**

conventional methods. It is proven that the proposed ACGS method has better capabilities in highlighting the brightness, contrast, and details of the resultant grayscale images. As a conclusion, the proposed ACGS method has successfully outperformed the conventional methods.

Quantitative analysis

In this section, four quantitative analyses are performed to further investigate the capability and the performance of the proposed color-to-grayscale conversion algorithm. The proposed method will be evaluated in terms of the computation complexity and its capabilities to highlight the brightness, contrast and the amount of details revealed by the resultant grayscale images. These analyses are employed to support the visual findings obtained from the qualitative analysis.

The first quantitative analysis used is the Mean Intensity (MI) test (Menotti et al., 2007; Kwok et al., 2009). The MI test is used to determine the mean brightness of the resultant grayscale images produced. The brighter resultant grayscale images will have higher values of *MI.* Consider a resultant grayscale image **J** = {*J(x, y)*}, with a total number of pixels of *T*, the *MI* values of this image is defined as follow:

$$MI = \frac{1}{T}\sum_{x=0}^{M-1}\sum_{y=0}^{N-1} J(x,y) \tag{14}$$

For *S* numbers of sample images used, the average mean intensity (*AMI*) value is defined as follow:

$$AMI = \frac{1}{S}\sum_{s=0}^{S} MI_s \tag{15}$$

The second quantitative analysis used is the standard deviation (SD) analysis (Menotti et al., 2007), which is used to measure the contrast of the resultant grayscale images. The grayscale images with greater *SD* values have greater contrast. The *SD* values of a given grayscale image with the probability density function (PDF) of *P*(*l*), where *l* represents the grayscale intensity levels of pixels, are defined as follows:

$$SD = \sqrt{\sum_{l=0}^{L-1}(l-\mu)^2 \times P(l)} \tag{16}$$

where, μ represents the mean intensity levels of the resultant grayscale images. For *S* numbers of sample images used, the average standard deviation (ASD) value is defined as:

$$ASD = \frac{1}{S}\sum_{s=0}^{S} SD_s \tag{17}$$

Next, the entropy (E) analysis (Kwok et al., 2009; Ooi and Mat-Isa, 2010a, b) is used to measure the richness of details revealed by a grayscale image. A grayscale image with higher value of *E* has richer details and greater detail-preserving capability. The *E* values of a given grayscale image with PDF of *P*(*l*), where *l* is the grayscale intensity levels of pixels are defined as follows:

$$E = -\sum_{l=0}^{L-1} P(l)\log_2 P(l) \tag{18}$$

For S numbers of sample images used, the average entropy (AE) value can be defined as follows:

$$AE = \frac{1}{S}\sum_{s=0}^{S} E_s \tag{19}$$

Finally, the last quantitative analysis carried out in this study is the average processing time, *t*. This analysis is employed to investigate the computational complexity of the proposed ACGS method in the real-time applications.

Based on the MI analysis result as shown in Table 1, the proposed ACGS method has higher capability in highlighting the brightness than the conventional methods. The proposed ACGS method produces the highest MI values for all images. These quantitative results support the visual inspection results performed in the previous subsection.

Next, for the *SD* analysis, the results reveal that the proposed ACGS method has better or comparable capability to highlight the contrast of resultant grayscale images as compared to the conventional methods. The proposed ACGS method produces three highest *SD* values for images named “Red Lanterns”, “Weave”, and

Table 2. Average quantitative measurement.

Algorithms	Single dominant color images			Low illumination color images		
	AMI	ASD	AE(bits)	AMI	ASD	AE(bits)
Averaging	87.86	40.652	6.9368	23.50	24.009	5.0727
NTSC	89.24	42.298	6.9625	23.84	24.843	5.0922
ACGS	**105.34**	**45.689**	**7.1259**	**24.80**	**25.256**	**5.1301**

Table 3. Average processing time.

Algorithms	Averaging	NTSC	ACGS
$t_{process}(ms)$	8.53	18.89	31.05

"Fruits". Although, the *SD* value produced by the proposed ACGS method is lower than the Averaging method in "Fishes", the visual inspection results in the previous subsection favor the proposed ACGS method. Finally, the results of the *E* analysis indicate that once again the proposed ACGS method has a better detail-preserving capability as compared to the conventional methods. All the *E* values produced by the proposed ACGS method are higher than those produced by the conventional methods

Besides using the images named "Red Lanterns", "Fruits", "Weave", and "Fruits" for the quantitative analysis, a total of 50 single dominant color images and 50 low illumination color images are used to further evaluate their average values of the mean intensity (AMI), standard deviation (ASD), and entropy (AE). These values are tabulated in Table 2. Meanwhile, the average processing time, $t_{process}$ of the proposed ACGS have been investigated as well. The average processing time of these three methods is tabulated in Table 3.

Based on Table 2, it reveals that generally the proposed ACGS method produces the highest AMI, ASD, and AE values for both the single dominant and low illumination color images. This shows that the proposed ACGS method in general has the better capabilities in highlighting the brightness, contrast, and details of the resultant grayscale images as compared to the conventional methods. These results are consistent with the visual inspection results performed in the previous subsection.

On the other hand, both the conventional methods outperform the proposed ACGS method in terms of the average processing time as shown in Table 3. However, the differences of the average processing time are not significant, which are 22.53 and 12.16 ms for the comparison between the proposed ACGS and Averaging methods, and the proposed ACGS and NTSC methods respectively. These differences can be compromised as the proposed ACGS performs a more detailed pixel distribution analysis on the input color images before the weight contribution values of R, G, and B components are determined. Unlike the proposed ACGS method, both the conventional methods assign an arbitrary weight contribution values to the R, G, and B components of the input color image without performing any analysis.

As a conclusion, the proposed ACGS method in general outperforms the conventional methods as it is able to produce the resultant grayscale images with higher level of brightness, contrast, and amount of details revealed. In addition, the computation complexity possessed by the proposed ACGS method is acceptable, which suggests that the potential of this proposed method to be implemented in the real-time processing applications.

Video processing analysis

In order to further investigate the capability of the proposed ACGS method in the real-time video processing application, the performance analysis of the proposed ACGS method in video processing is performed. Similar to the digital still images, the capabilities of the proposed ACGS method in video processing are also evaluated qualitatively and quantitatively.

For the qualitative analysis, the capability of the proposed ACGS method will be evaluated through the naked eye. Six consecutive input video frames are extracted from the video sample. These original frames and their resultant grayscale frames are illustrated in Figure 8.

For the qualitative analysis, a total of 50 video samples are prepared using a video-capturing algorithm. The video-capturing algorithm is implemented using Borland C++ Builder and Video Lab component on a Core 2 Duo 2.00 GHz CPU. Each of these video samples is a short video clip with the running time duration of 10 sec. For each video sample, the mean capturing time required to capture each frame, $t_{capture}$ will be calculated based on the number of frames captured within 10 seconds as follows:

$$t_{capture} = \frac{Duration\ \ of\ \ video}{Number\ \ of\ \ frames\ \ in\ \ video\ \ clip} \quad (20)$$

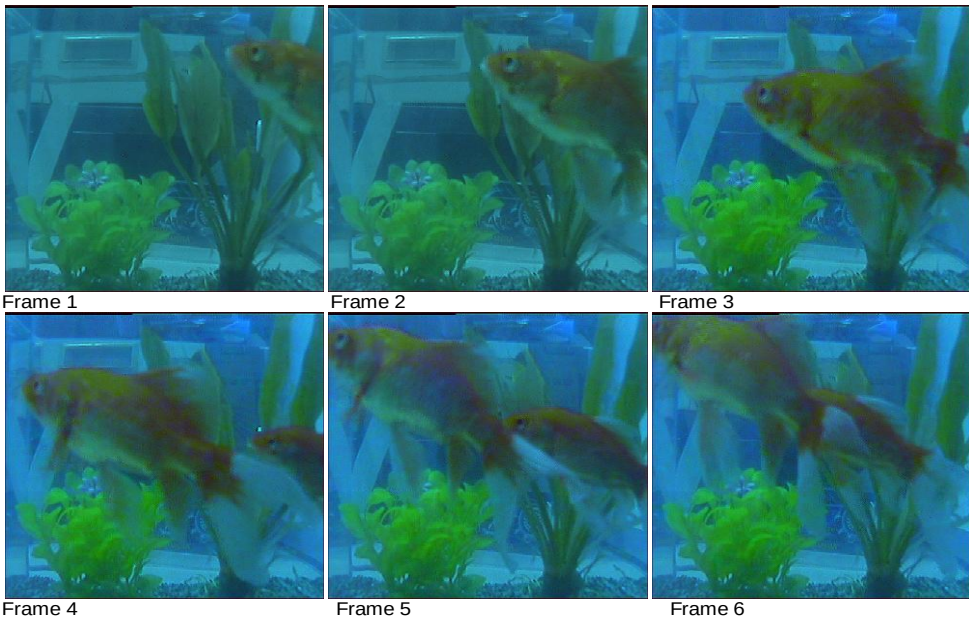

Figure 8a. Six frames from video (The original frames).

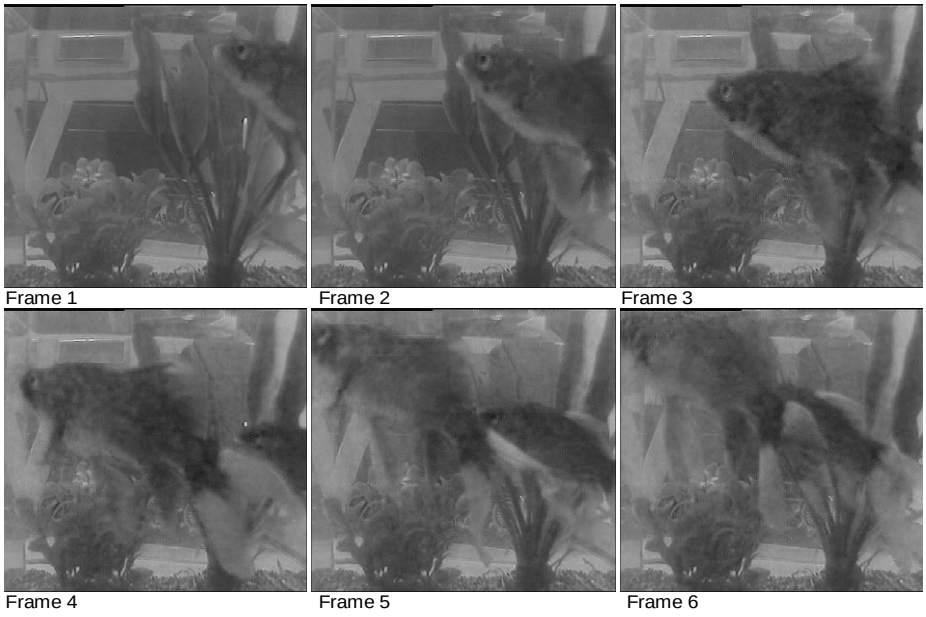

Figure 8b. Six frames from video (The resultant grayscale frames after applying the proposed ACGS method).

For S number of samples used, the average mean capturing time, $\bar{t}_{capture}$ is defined as:

$$\bar{t}_{capture} = \frac{1}{N}\sum_{j=1}^{S}(t_{capture})_j \quad (21)$$

Meanwhile, the mean processing time required to process each frame for a given video sample, $t_{process}$ is calculated as:

$$t_{process} = \frac{1}{N}\sum_{k=1}^{N} t_{process\ k-th\ \ frame} \quad (22)$$

where, N represents the total number of frames in each

Table 4. Quantitative measurement of video processing analysis.

$\bar{t}_{process}$ **(ms)**	$\bar{t}_{capture}$ (ms)	$SD_{capture}$	$SD_{process}$
63.86	38.84	0.00215	0.00076

video clip sample and $t_{process\ k\text{-}th\ frame}$ represents the processing time required for each *k*-th frame. For *S* number of samples, the average mean processing time, $\bar{t}_{process}$ is defined as:

$$\bar{t}_{process} = \frac{1}{S}\sum_{j=1}^{S}(t_{process})_j \quad (23)$$

Besides calculating the $\bar{t}_{capture}$ and $\bar{t}_{process}$, the sample standard deviation analysis is also performed to evaluate the performance consistency of the proposed ACGS method in the video processing applications. The sample standard deviation of the mean capturing time, $SD_{capture}$ is used to investigate the stability of the video-capturing algorithm in capturing the input frames. Meanwhile, the sample standard deviation of the mean processing time, $SD_{process}$ is used to evaluate the consistency of the proposed ACGS method in processing the input video frames. Smaller value of $SD_{process}$ indicates that the proposed ACGS method is able to perform consistently in various types of input video with small variation of the mean processing time. For *S* number of samples, both the $SD_{capture}$ and $SD_{process}$ are defined as such:

$$SD_{capture} = \sqrt{\frac{1}{S-1}\sum_{j=1}^{S}\left[(t_{capture})_j - \bar{t}_{capture}\right]^2} \quad (24)$$

$$SD_{process} = \sqrt{\frac{1}{S-1}\sum_{j=1}^{S}\left[(t_{process})_j - \bar{t}_{process}\right]^2} \quad (25)$$

The values of $\bar{t}_{capture}$, $\bar{t}_{process}$, $SD_{capture}$, and $SD_{process}$ for the 50 video samples are calculated using the Borland C++ Builder on a Core 2 Duo 2.00 GHz CPU. The results of the abovementioned quantitative measurement are tabulated in Table 4.

Based on the results tabulated in Table 4, it reveals that $\bar{t}_{process}$ of the proposed ACGS method is significantly smaller than $\bar{t}_{capture}$ of the video capturing algorithm. The smaller value of $\bar{t}_{process}$ is favored as it ensures the resultant grayscale videos are displayed smoothly without any lagging problem surfacing. Meanwhile, the $SD_{process}$ of the proposed ACGS method has outperformed the $SD_{capture}$ of the video capturing algorithms as well. The smaller value of $SD_{process}$ ensures the robustness of the proposed ACGS method in the real-time video processing applications as it is able to process the input video frames with small variation of processing times. The above mentioned video processing analysis of results demonstrate that the proposed ACGS method is feasible to be applied in the real-time video processing application as it has a short processing time and it is able to perform consistently during the color-to-grayscale conversion process.

Conclusion

In this paper, a new Adaptive Color to Grayscale (ACGS) conversion algorithm is introduced. The proposed ACGS method determines the weight contribution values of R, G, and B components for a given color image adaptively during the color-to-grayscale conversion process. The experimental results have proven that the proposed ACGS method is able to produce resultant grayscale images with higher level of brightness, contrast, and amount of details revealed as compared to the conventional methods. In addition, the video processing analysis has revealed the excellent performance of the proposed ACGS method in the real-time video processing applications. Therefore, the proposed ACGS method is suitable to be implemented as both the pre- and post- processing techniques of digital images for display and to be applied in various printing systems.

ACKNOWLEDGEMENT

The authors would like to express their sincere thanks to the associate editor and all reviewers who made great contributions to the improvement of the final paper. This research was supported by the Fundamental Research Grant Scheme (FRGS) entitled “Investigation of New Color Image Illumination Estimation Concept for Development of New Color Correction Techniques” and Universiti Sains Malaysia (USM) Postgraduate Fellowship Scheme.

REFERENCES

Bala R, Braun K (2004). Color-to-grayscale conversion to maintain discriminabillity. In: Proceed. Soc. Photogr. Instrum. Eng. pp. 196-202.

Bala R, Eschbach R (2004). Spatial color-to-grayscale transformation preserving chrominance edge information. In: 12th Color Imaging Conf.: Color Sci. Eng. Syst. Technol. Appl. Scottsdale, AZ, pp. 82-86.

Cadik M (2008). Perceptual evaluation of color-to-grayscale image conversions. Comp. Graph. Forum. 27(7):1745-1754.

Dikbas S, Arid T, Altunbasak Y (2007). Chrominance edge preserving grayscale transformation with approximate first principal component for color edge detection. In: IEEE Int. Conf. Image Process. 2007 (ICIP 2007), pp. I - 261 - II – 264.

Gonzalez RC, Woods RE (2002). Digital image processing. Prentice Hall.

Gooch A, Tumblin J, Gooch B (2005). Color2gray: Salience-preserving colour removal. ACM T. Graphic 24(3):634-639.
Grundland M, Dodgson NA (2007). The decolorize algorithm for contrast enhancing, color to grayscale conversion. Technical Report UCAM-CL-TR-649, University of Cambridge.
Kekre HB, Thepade SD (2009). Improving `color to gray and back' using kekre's luv color space. In: IEEE Int. Adv. Comput. Conf. (IACC), pp. 1218-1223.
Kwok NM, Ha QP, Dikai L, Gu F (2009). Contrast enhancement and intensity preservation for gray-level images using multiobjective particle swarm optimization. IEEE T. Autom. Sci. Eng. 6(1):145-155.
Lu J, Plataniotis KN (2009). On conversion from color to gray-scale images for face detection. In: IEEE Comput. Soc. Conf. Comput. Vis. Pattern Recognit. (CVPR) Workshop, pp. 114-119.
Menotti D, Najman L, Facon J, Araujo AdA (2007). Multi-histogram equalization methods for contrast enhancement and brightness preserving. IEEE T. Consum. Elect. 53(3):1186-1194.
Ooi CH, Mat-Isa NA (2010a). Adaptive contrast enhancement methods with brightness preserving. IEEE T. Consum. Elect. 56(4):2543-2551.
Ooi CH, Mat-Isa NA (2010b). Quadrants dynamic histogram equalization for contrast enhancement. IEEE T. Consum. Elect. 56(4):2552-2559.
Rasche K, Geist R, Westall J (2005). Detail preserving reproduction of color images for monochromats and dichromats. IEEE Comput. Graph. 25(3):22-30.
Smith K, Landes PE, Thollot J, Myszkowski K (2008). Apparent greyscale: A simple and fast conversion to perceptually accurate images and video. Comp. Graph. Forum. 27(2):193-200.